Study on sawtooth collapses using two-fluid equations

Q. Yu, S. Günter and K. Lackner

Max-Planck-Institut für Plasmaphysik, 85748 Garching, Germany

1. Introduction

As a typical phenomenon observed in tokamak discharges, sawtooth collapse has attracted much research interest [e.g. 1-7]. Using the large aspect-ratio tokamak approximation, sawtooth collapses are studied here numerically based on two fluid equations, including the electron continuity equation, generalized Ohm's law, the equation of motion in the parallel and the perpendicular direction (after taking $\mathbf{e}_t\cdot\nabla\times$), and the electron energy transport equation [8],

$$\frac{dn_e}{dt} = d_1\nabla_{||}j - \nabla_{||}(n_e v_{||}) + \nabla\cdot(D_\perp\nabla n_e) + S_n \quad (1)$$

$$\frac{d\psi}{dt} = E_0 - \eta j - \frac{\eta}{\nu_{ei}}\frac{dj}{dt} + \eta\frac{\mu_e}{\nu_{ei}}\nabla_\perp^2 j + \Omega(\nabla_{||}n_e + \nabla_{||}T_e) \quad (2)$$

$$\frac{dv_{||}}{dt} = -C_s^2\nabla_{||}p / n_e + \mu\nabla_\perp^2 v_{||} \quad (3)$$

$$\frac{dU}{dt} = S^2\nabla_{||}j + \mu\nabla_\perp^2 U \quad (4)$$

$$\frac{3}{2}n_e\frac{dT_e}{dt} = d_1T_e\nabla_{||}j - T_e n_e\nabla_{||}v_{||} + n_e\nabla\cdot(\chi_{||}\nabla_{||}T_e) + n_e\nabla\cdot(\chi_\perp\nabla_\perp T_e) + S_p \quad (5)$$

where the magnetic field $\boldsymbol{B}=B_{0t}(\boldsymbol{e}_t-\boldsymbol{e}_\theta k_t/k_\theta)+\nabla\psi\times\boldsymbol{e}_t$, ψ is the helical flux function, k_θ=m/r and k_t=n/R, m and n are the poloidal and toroidal mode numbers, r and R the minor and major radius, and the subscript 0 denotes an equilibrium quantity. The ion velocity $v=v_{||}\boldsymbol{e}_{||}+\boldsymbol{v}_\perp$, $\boldsymbol{v}_\perp=\nabla\phi\times\boldsymbol{e}_t$, ϕ is the stream function, the subscripts || and $\perp$ denote the parallel and perpendicular components, $d/dt=\partial/\partial t+\boldsymbol{v}_\perp\cdot\nabla$, j is the plasma current density along the $\mathbf{e}_t$ direction, $U=-\nabla_\perp^2\phi$ the plasma vorticity, μ the ion viscosity, χ the heat conductivity, and D the particle diffusivity. S_n and S_p are the particle and heat source, E_0 is the equilibrium electric field, $S=\tau_R/\tau_A$, $p=p_e=n_eT_e$, $d_1=\omega_{ce}/\nu_{ei}$, $\Omega=\beta_e d_1$, $C_s=[T_e/m_i]^{1/2}/(a/\tau_R)$, $\beta_e=4\pi n_eT_e/B_{0t}^2$, ω_{ce} is the electron cyclotron frequency, μ_e the perpendicular electron viscosity, υ_{ei} the electron-ion collisional frequency, $\tau_A=a/V_A$, and V_A is defined using B_{0t}.

2. Numerical results

Typical ASDEX Upgrade plasma parameters, B_{0t}=2T, a=0.5m, R=1.7m, T_e=2keV and $n_e=3\times10^{19}m^{-3}$ at q=1 surface, are utilized, leading to $S=2.6\times10^8$, $\Omega=9.4\times10^4$, $C_s=2.0\times10^7(a/\tau_R)$, $d_1=3.1\times10^7$, and $\nu_{ei}=2.2\times10^4$/s. Furthermore, $\mu_e/\upsilon_{ei}=10^{-4}a^2$, $\chi_\perp=\mu_\perp=0.2/m^2/s=19(a^2/\tau_R)$,

$D_\perp=\mu/5$, $\chi_\parallel/\chi_\perp=8.0\times10^8$, and a monotonic profile for the safety factor q is assumed, with $q_0=0.91$ and $r_{q=1}=0.3a$, where q_0 is the original safety factor at r=0, and $r_{q=1}$ the minor radius of the q=1 surface. The original equilibrium electron temperature profile has the form $T_e=T_{e0}[1-(r/a)^2]^\kappa$, and the equilibrium electron density profile is taken to be a constant.

In figure 1 the time evolution of the helical flux during the sawtooth collapse at the x- and the o-point of the island as well as at the original magnetic axis are shown for $\kappa=2$. The helical flux at the x-point varies from that at the island's o-point to that at the axis, indicating a full magnetic reconnection. The reconnection process takes a time period less than $100\mu s$ ($1\,\tau_A=8.7\times10^{-8}$ s) when neglecting the small flux change in the early phase, in agreement with ASDEX Upgrade experimental results [2].

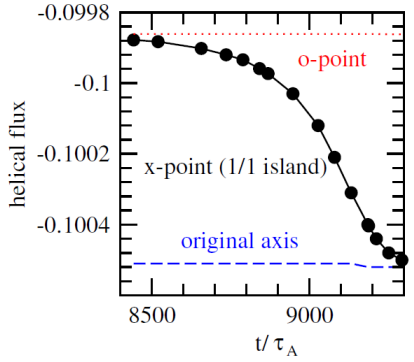

Figure 1 Time evolution of the helical flux at the x- and the o-point of the island as well as at the original magnetic axis for $\kappa=2$.

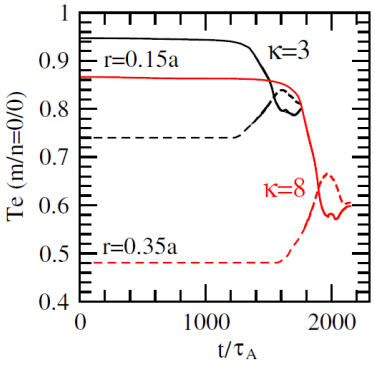

Figure 2 Time evolution of the electron temperature at the minor radius both inside and outside the $q=1$ surface for $\kappa=3$ and 8.

The time evolution of the electron temperature during the sawtooth collapses at the minor radius both inside and outside the $q=1$ surface is shown in figure 2 for $\kappa=3$ and 8. When the island width is still small, the island growth is faster for a smaller value of κ (or electron diamagnetic drift frequency ω_{*e0}) due to a weaker stabilizing effect of the diamagnetic drift. However, a fast decrease in the electron temperature is found for both cases once the island width is sufficiently large. This can be explained by the flattening of the electron temperature profile inside a large island.

Slow sawtooth collapses are found only for a sufficiently small $(1-q_0)$ and a large local ω_{*e0} at the $q=1$ surface. Figure 3 shows the time evolution of the electron temperature both inside and outside the $q=1$ surface for $q_0=0.95$ and $r_{q=1}=0.21a$. In this case, a much longer collapse time, $\sim 10^4\,\tau_A \sim 10^{-3}s$, is found for $\kappa=4$ and 6. In the hybrid operational mode with a small $(1-q_0)$ and weak magnetic shear in the central region, slow sawtooth collapses or even continuous $1/1$ mode activity were observed in experiments [3,4].

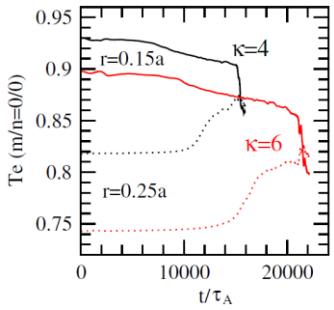

Figure 3 Time evolution of the electron temperature both inside and outside the $q=1$ surface for $q_0=0.95$, $r_{q=1}=0.21a$ and $\kappa=4$ and 6.

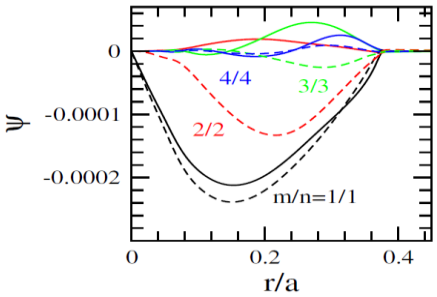

Figure 4 Radial profiles of the normalized (to aB_{0t}) helical flux functions $\psi_{1/1}$, $\psi_{2/2}$, $\psi_{3/3}$ and $\psi_{4/4}$ for the simulation of figure 1 at the time $t=8919\,\tau_A$.

The amplitudes of high harmonic perturbations are usually found to be comparable to that of the 1/1 component during the collapse, as seen in experiments [2]. Fig. 4 shows the radial profiles of the normalized (to aB_{0t}) flux functions $\psi_{1/1}$, $\psi_{2/2}$, $\psi_{3/3}$ and $\psi_{4/4}$ for the simulation of figure 1 at the time $t=8919\,\tau_A$. The solid (dashed) curves represent the real (imaginary) part.

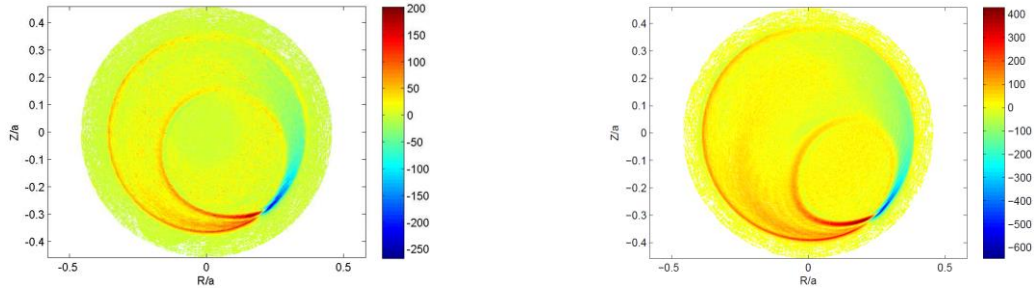

Figure 5 Contours of negative parallel electric field, $-E_{\parallel}=d\psi/dt$ (in the unit aB_{0t}/τ_R), at $t=8851$ (left) and $8956\,\tau_A$ (right). R=0 corresponds to the major radius of the original magnetic axis, and Z is along the vertical direction. The parallel electric field is increased during the collapse by *1000* times in the island's x-point region.

During the sawtooth collapse, strong parallel electric field is induced. Corresponding to Fig. 1, contours of the negative parallel electric field, $-E_{\parallel}=d\psi/dt$ (in the unit aB_{0t}/τ_R), are shown at $t=8851$ and $8956\,\tau_A$ in figure 5. The original equilibrium electric field is $-0.55(aB_{0t}/\tau_R)$. The parallel electric field is increased during the sawtooth collapse compared to the equilibrium field by about *1000* times in the island's x-point region. The maximum electron velocity produced by the reconnection is found to be $1.05*10^8 m/s$, corresponding to an electron energy of *31.6 keV* and a collision time of *1.3 ms*. This indicates that supra-thermal electrons can be generated during the sawtooth collapse in existing tokamak plasmas as observed in experiments [5,6]. As the generated fast electron energy is proportional to $(aB_{0t})^2$, relativistic runaway electrons could readily be generated during sawtooth collapses in ITER.

In figure 6 the linear mode growth rate and mode frequency are shown as a function of the local ω_{*e0}, obtained for $C_s=\mu_e=0$ and zero electron inertia. The mode is stable for a sufficiently

large ω_{*e0} due to the stabilization by diamagnetic drift. The mode frequency does not linearly increase with ω_{*e0}. The difference between these two frequencies leads to a plasma current density perturbation being out of phase with ψ, resulting in an $m/n=0/0$ component electromagnetic torque $r\cdot\boldsymbol{j}\times\boldsymbol{B}$, localized around the $q=1$ surface as shown in figure 7 in the linear phase for $\omega_{*e0}=5.0\times10^4\,\tau_R$. The driven plasma rotation is in the counter (co-) current direction inside (outside) the $q=1$ surface in the linear phase, propagates towards the magnetic axis during the nonlinear phase and reverses the rotation direction after the sawtooth collapse, in agreement with TCV experimental observations [7]. The amplitude of the driven rotation velocity reaches the level of the electron diamagnetic drift velocity.

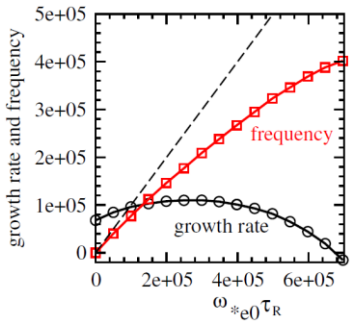

Figure 6 Linear mode growth rate and frequency versus the local $\omega_{*e0}\tau_R$ at the $q=1$ surface.

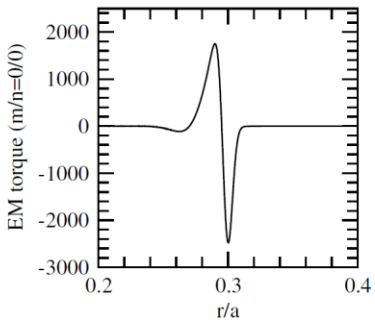

Figure 7 Radial profile of the m/n=0/0 component electromagnetic torque $r\cdot\boldsymbol{j}\times\boldsymbol{B}$ in linear phase.

3. Summary

(a) Based on two-fluid equations, fast sawtooth collapse, ~100μs or shorter, is obtained for typical ASDEX Upgrade parameters, in agreement with experimental observations. Slow collapses are also found for small values of $(1-q_0)$ and large local diamagnetic drift frequencies. (b) During the sawtooth collapse, strong parallel electric field is formed in the x-point region of the magnetic island, which could generate super-thermal electrons in existing tokamaks and runaway electrons in ITER.

[1] S. Von Goeler *et al.*, Phys. Rev. Lett. **33** (1974) 1201.

[2] V. Igochine, J. Boom, I. Classen *et al.*, Plasmas **17**, 122506 (2010).

[3] P. Buratti, B. Alper, S.V. Annibaldi, *et al.*, Plasma Phys. Control. Fusion, **48**, 1005 (2006).

[4] J. Stober, A.C.C. Sips, C. Angioni, *et al.*, Nucl. Fusion **47**, 728 (2007).

[5] P. V. Savrukhin, Phys. Rev. Lett. 8**6** (2001) 3036.

[6] I. Klimanov, *et al.*, Plasma Phys. Control. Fusion, **49**, L1-L6 (2007).

[7] B. P. Duval, *et al.*, Phys.Plasmas **15**, 056113 (2008); 23rd IAEA FEC (2010), IAEA-CN-180.

[8] Q. Yu, Nucl. Fusion **50**, 025014 (2010).